

Mechanical Deformation and Electrical Breakdown of PEN at High Electric Fields

Ahmed Lotfy,* José Fidel Chávez-Lara,† Laurent Boudou, Juan Martinez-Vega

Université Paul Sabatier, Laboratoire de Génie Electrique (UMR CNRS 5003), 118 Route de Narbonne, 31062 Toulouse, Cedex, France

Received 18 May 2006; accepted 1 May 2007

DOI 10.1002/app.26775

Published online 9 August 2007 in Wiley InterScience (www.interscience.wiley.com).

ABSTRACT: In this work, samples of amorphous and semicrystalline PEN (polyethylene-2,6-naphthalene dicarboxylate) were subjected to DC electric fields for different durations up to their dielectric breakdown, with or without depolarization. The field-induced mechanical strains in the samples were studied by means of a nondestructive optical technique without resorting to any physical contact. The results showed that amorphous samples were more vulnerable to the field-induced mechanical deformation when compared with similar semicrystalline samples. However, both morphologies showed in some samples contradictory behavior at prebreakdown field strength, some caused yielding of the polymer while the others seemed to have the opposite effect. In the latter category,

yet some showed the maximum yield point at a particular critical field starting from which the deformation began to diminish significantly to reach a total cancellation at the breakdown field. This critical field quantified at 260 kV/mm is probably a pronouncement of critical ageing and breakdown in PEN. The deformation seems to be an evolution very similar to the evolution of DC current at high fields. Furthermore, the varying response of the samples implies further work to be undertaken to validate a clear mechanism. © 2007 Wiley Periodicals, Inc. *J Appl Polym Sci* 106: 2963–2969, 2007

Key words: PEN thin films; electromechanical response; high electric field

INTRODUCTION

The mechanical response of polymer films subjected to high electric fields gained early interest in the literature,^{1–8} in view of improving the comprehension of phenomena that lead to the electric breakdown. However, the progress in this field has been associated with nonnegligible economic consequences. Their origins could be attributed to electronic, thermal, or mechanical mechanisms.

Nevertheless, the adoption of noncontact strain measurement methods^{9,10} was decided upon to obtain accurate deformation levels, and these methods do not require any physical contact with the samples under study so as not to affect the measurement accuracy.

They were already tried to assess the mechanical response of polyethylene terephthalate (PET) subjected to increasing electrical fields.² It was established

experimentally that these electrical stresses were responsible for localized mechanical deformation.

In this work, the mechanical response of PEN (polyethylene-2,6-naphthalene dicarboxylate) films under applied electric field is investigated. The different properties of PEN were subjects of several studies during the last few years.^{11–14} In our study, we detected far more important field-induced mechanical deformation in the amorphous morphology than in the semicrystalline one. The deformation in amorphous variety is found to be four times larger than that in the semicrystalline variety.

The crystallinity and, in particular, the type of crystallite (β) developed at the surface which increase the rigidity of PEN are apparently the basis of this difference. The superior molecular mobility under electric field gives a shorter threshold field initiating the deformation than in semicrystalline PEN. There is, as a result of the field-induced mechanical forces, an instability in the polymer morphology, mainly as conformational changes in the amorphous phases and in other interrelated processes such as the extension of tied molecules between two lamellae and the formation of microvoids. These processes invariably affect the aging and the breakdown behavior.

Good indicators have been published in high field behavior which shows high current slopes of 16.5 in the I(F) characteristics.¹⁵ However, the field-induced

Correspondence to: L. Boudou (laurent.boudou@get.ups-tlse.fr).

*Permanent address: Electrical and Computer Control Engineering Department, Faculty of Engineering and Technology, Arab Academy for Science & Technology & Maritime Transport, Abu Kir, Alexandria, Egypt.

†Permanent address: Instituto Tecnológico de Chihuahua, Chihuahua, México.

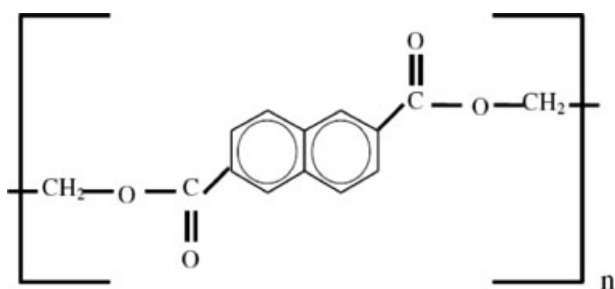


Figure 1 Chemical formula of PEN (polyethylene-2,6-naphthalene dicarboxylate).

strain response remains the one possibility which is more and more investigated to clarify the breakdown behavior. Our data of those steep currents at high fields are an important link to tie up our results in this study, probably because the Maxwell pressure exerted by the electrodes has an influence on the charge carriers, the aging, and the breakdown. The values of threshold field starting the mechanical deformation as well as extremely high currents¹⁵ are found to be very similar in their evolution at high fields.

The relationship between these two indicators was analyzed and, in particular, the yielding evolution in each morphology. Finally, the mechanical deformation was analyzed during breakdown.

MATERIAL

The molecular structure of PEN is shown in Figure 1. This polymer is a double aromatic ring polyester characterized by its excellent mechanical properties as compared to its competitors such as the PET. Its Young's modulus is 25% greater than that of PET (5200 MPa vs. 3900 MPa) at the room temperature and much greater from 100 to 150°C. The samples of PEN used in our experimental work were provided by Dupont de Nemours, Luxembourg, (25 μm amorphous and semicrystalline PEN).

Differential scanning calorimetry (DSC) was used to ensure the morphology status of the samples provided. The analyses were carried out in nitrogen liquid with specimens of about 13 mg by subjecting them to a rise in temperature from 30 to 290°C at 10°C/min. This technique allows us to determine the glass transition (T_g) and the melting point (T_m) temperatures of the sample (Fig. 2). The knowledge of crystallization (ΔH_c) and melting (ΔH_m) enthalpies of sample allows direct calculation of the crystallinity rate ($\chi(\%)$), as follows:

$$\chi(\%) = 100 \left(\frac{\Delta H_m - \Delta H_c}{\Delta H_\infty} \right)$$

where $\Delta H_\infty = 103.4 \text{ J/g}$, and is the melting enthalpy of fully crystalline PEN.

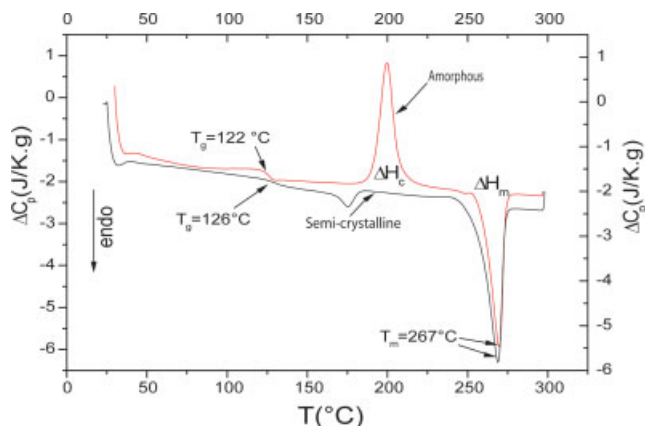


Figure 2 DSC thermograms of the amorphous ($\chi < 1\%$) and semicrystalline ($\chi \approx 44\%$) PEN. [Color figure can be viewed in the online issue, which is available at www.interscience.wiley.com.]

Figure 2 also shows a slight jump in specific heat $\Delta C_p \text{ (J g}^{-1} \text{ K}^{-1}\text{)}$ of the amorphous sample, which corresponds to the glass transition (122°C). In the semicrystalline sample, this temperature is a little bit greater (126°C). The melting temperatures are the same, 267°C in both the samples.

To guarantee a better electrode/polymer contact and consequently attenuate corona discharges, samples were metalized by gold coating using a S150B plasma sputter coater. Electrodes of 20 mm diameter and 30 nm thickness were thus obtained on both faces. The prepared samples were then short-circuited for 30 min to eliminate the initial charges existing on the faces before applying the experimental procedure.

EXPERIMENTAL SETUP

Figure 3 shows the set up of the experimental device used to measure the mechanical response of PEN films. This one includes four fundamental parts:

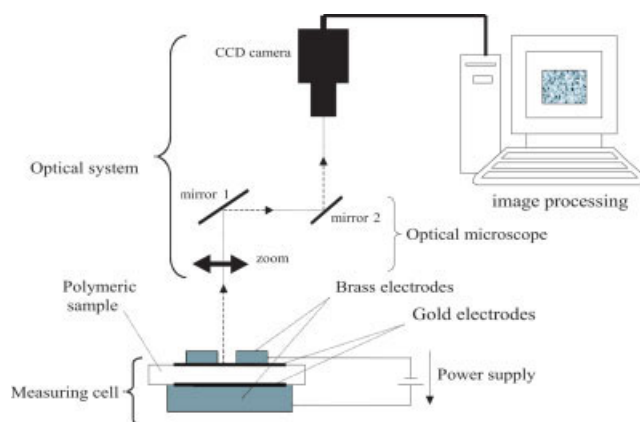


Figure 3 Experimental setup. [Color figure can be viewed in the online issue, which is available at www.interscience.wiley.com.]

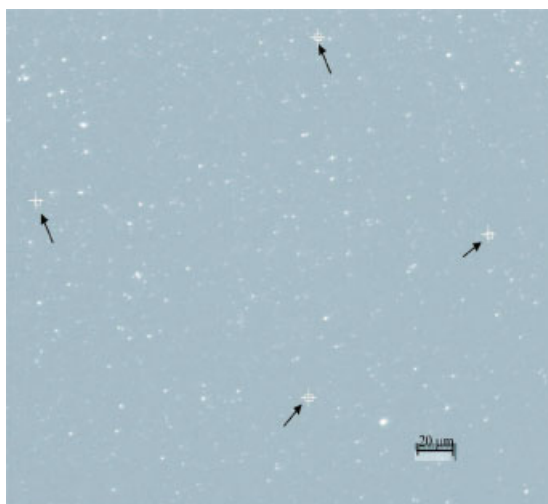


Figure 4 Little contrasting spots at the metalized surface of PEN and markers of initial reference. [Color figure can be viewed in the online issue, which is available at www.interscience.wiley.com.]

- The sample holder cell: The sample to be tested is placed between its two external brass electrodes. The upper one, the negative, is constructed as a hollow cylinder of 12 mm diameter. This permits the use of a flexible light source to illuminate the upper face of the sample. The lower electrode, the positive one, is connected to a high DC voltage source.
- A high DC voltage source (HCN 35-20000; 20 kV and 1.5 mA limited current) with controllable output.
- An optical system which is formed by an optical microscope connected to a CCD (charge coupled device) camera.
- A computing system which permits the data processing from the camera.

The CCD camera (768 by 576 pixels and 256 gray levels) is mounted above the optical microscope which is used to capture the image of the gold metalized surface of the sample. This is composed of small contrasting spots which represent the microscopic light contrast of traditional metalization defects in the sample as shown in Figure 4. Four different spots are selected and marked by means of the software used (Fig. 4). Indeed, we are able in this way to track the four spots of the sample surface in order to quantify in real time the field-induced mechanical strain. So, when a step voltage is applied to the sample, the markers are moved due to the field-induced mechanical deformation. The computer follows up the successive positions of the markers giving us the possibility of calculating the field-

induced mechanical strain. A good description of this process is given in Ref. 3 along with the principle of the strain measurement, ε_1 and ε_2 associated with the principal directions of the local sample surface are the main components of the deformation vector whose modulus (ε) is calculated as follows:

$$\varepsilon = (\varepsilon_1^2 + \varepsilon_2^2)^{1/2}$$

It is important to note that we assumed the homogeneity of the deformation for the measurement, and as a result, these values are average values. The mechanical measurements were performed as a function of time and then analyzed with respect to the applied electric field to determine the induced mechanical deformation-electric field $\varepsilon(F)$ characteristics of the amorphous and semicrystalline PEN.

RESULTS

Measurements were carried out at the room temperature at atmospheric pressure and for very short durations (less than 30 min) in order to minimize the influence of the environmental conditions. Several protocols of DC electric stress application were adopted, and the differences consisted in the duration of DC voltage application and/or the existence of a depolarization period.

To assess the level of deformation resulting from high DC voltage application, PEN samples were stressed for periods of 5, 10, 15, and 30 min followed by a similar depolarization period at every voltage level. Figure 5 shows the resulting deformation of a semicrystalline 25- μm sample stressed by 2.3, 3.6, and 4.6 kV respectively, with CCD camera sampling rates of one photo per three seconds. The depolarization periods were omitted for demonstration.

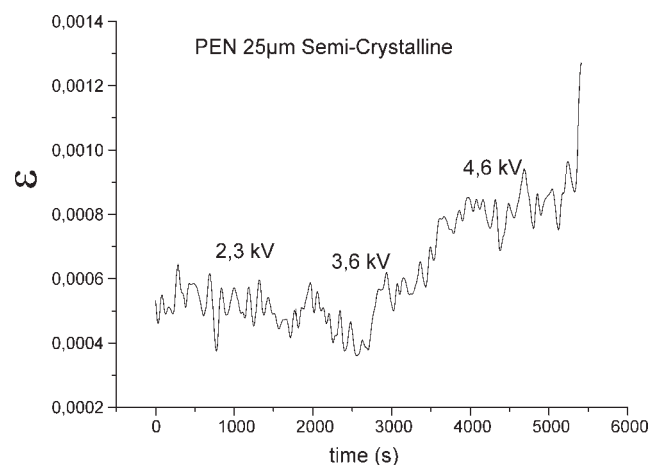


Figure 5 Induced mechanical deformation of semicrystalline PEN samples.

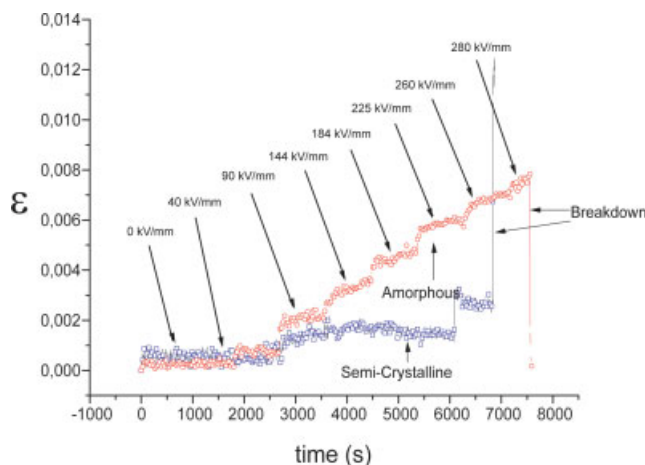


Figure 6 Induced mechanical deformation versus time; 15 min of field application. [Color figure can be viewed in the online issue, which is available at www.interscience.wiley.com.]

The deformation becomes relatively appreciable starting from 3.6 kV (144 kV/mm) for the adopted duration of electric stress application. Below this level, it is hard to differentiate between signal and noise. This onset of clear deformation was reproducible for other samples as well, under conditions of the same stress durations.

Figure 6 shows the total deformation for a stress application duration of 5 min at each step of electric stress without any depolarization period. In the amorphous case, the deformation starts being remarked at 2300 V (92 kV/mm).

Also, it shows the deformation versus voltage application duration for both semicrystalline and amorphous samples subjected to 15-min periods of stress as well as of depolarization. The response during the depolarization period is omitted in order to demonstrate the increased deformation at higher stress levels. The maximum deformation levels attained for most of the tested semicrystalline samples were of the order of 0.002 (the resolution of this technique is better than 10^{-4}), while those attained for amorphous samples were four times bigger, 0.008, a foreseeable result in view of the crystallinity and the crystallites (β) developed at the surface. This morphology increases the stiffness of the polymer, and hence its mechanical properties. Their breakdown fields are 260 and 300 kV/mm, respectively.

Figure 7 shows the deformation of semicrystalline PEN sample subjected to different DC electric fields for 30 min at each field level. The breakdown field corresponds to 300 kV/mm. Although the deformation levels in either semicrystalline or amorphous samples were reproducible for most of the tested samples; the breakdown mechanism seemed to be rather complex.

A marked rise in currents and the onset of electroluminescence are proposed as practical indicators.^{15,16} However, it is suggested in the literature⁴ that it could be indicators of other important processes induced by the electrical field, which may not directly involve electrons. In this way, the field-induced compressive stress can generate conformational changes in the polymer morphology. Moreover, this mechanical stress will increase as proportional to the square of the electric field, $\frac{\epsilon E^2}{2}$, so as to enhance thermally-induced bond breaking. Thus, both processes are frequently associated with aging and breakdown.

Nevertheless, the breakdowns in the case of the amorphous sample in Figure 6 and the semicrystalline one in Figure 7 show a reduction in the deformation, which suggests a thermally dominated mechanism attributed to the propagation of local breakdowns caused by large local fields in microvoids. The mechanisms of electro-fracture and filamentary electromechanical breakdown do not conform to this behavior because instead of the yielding of the polymer they seem to recover their elastic energy. The possible explanation of the phenomenon is an uncompensated thermal or kinetic energy. It is rather a mechanism of electrical aging having a mechanical origin.^{2,3} This could be highlighted by the measurement of the defect-trap density (scission and reorganization of chemical bonds in new conformations), supposedly higher under aging conditions. Besides, considering the origin of electrical aging by space charge amongst other possibilities, this theory could be concordant with our results, especially in the case of the amorphous one where an elevated charge density is remarked, whereas it is not completely clear in the case of semicrystalline in which the charge density remains rather low.¹⁷

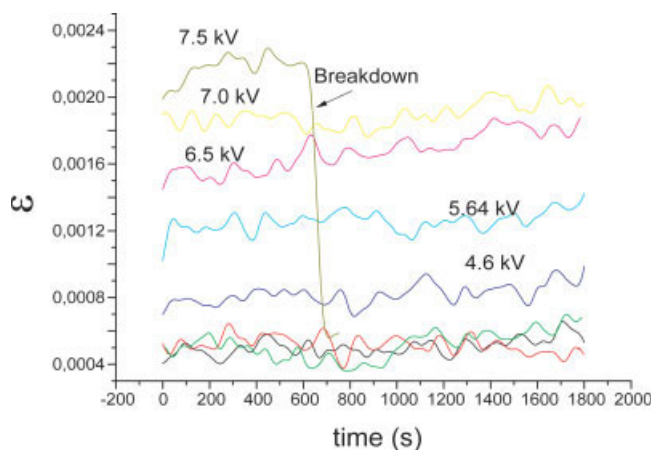


Figure 7 Induced mechanical deformation of semicrystalline PEN (25 μ m); 30 min of field application. [Color figure can be viewed in the online issue, which is available at www.interscience.wiley.com.]

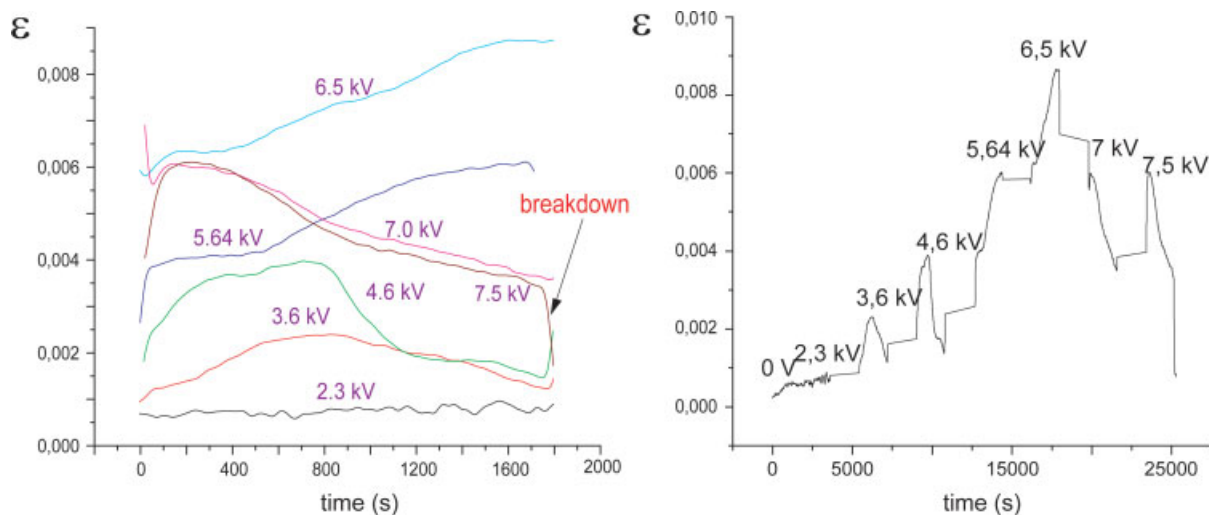


Figure 8 Induced mechanical deformation of amorphous PEN (25 μm); 30 min of field application. [Color figure can be viewed in the online issue, which is available at www.interscience.wiley.com.]

However, an outstanding current rise is observed at the same field levels (almost in the range of microamperes)¹⁵ where a mechanism of ionization by impact could be the precursor. Thus, the possibility of an avalanche breakdown mechanism, source of electrical trees, and subsequent breakdown, should remain open.

On the other hand, in the case of the semicrystalline sample of Figure 6, the breakdown is mostly electromechanical resulting from an imbalance between electrostatic compression (exerted by the electrodes which stress the sample) and the buildup of the uncompensated elastic energy, in such a way that the polymer yields to the pressure. This latter result may be considered to be in accordance with the model proposed by Forthergill,^{6,7} where the disproportion causes a filamentary crack to propagate

through the polymer film. This model predicted the breakdown strength field as proportional to the 4th root of Young's modulus, $F_{\text{Breakdown}} \propto Y^{1/4}$. In PEN, the Young's modulus is 5200 Mpa corresponding to a breakdown field of 268 kV/mm with the model application. This value is very close to the real breakdown values in this polymer, 300 kV/mm \pm 40. In addition, if the material is viscoelastic, as the majority of polymers, a progressive reduction in the thickness of the sample can take place. The application of an electrical field will generate a mechanical pressure which can be significant when the field approaches the breakdown value. Nevertheless, the lack of reproducibility of breakdown in similar samples tested under the same conditions and yielding the same deformation levels suggests that both mechanisms are partially operating.

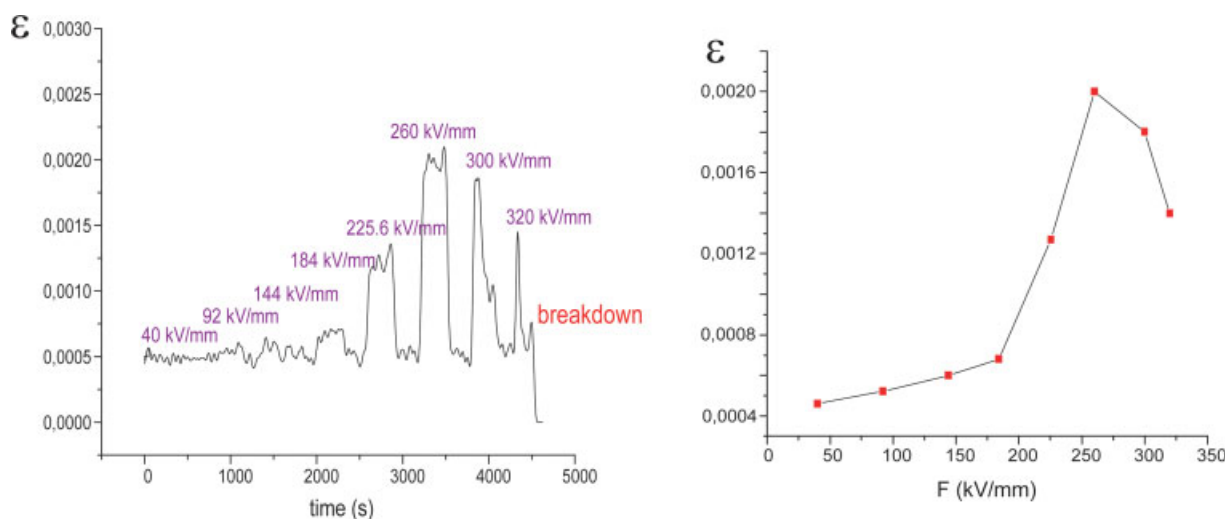


Figure 9 Induced mechanical deformation of semicrystalline PEN (25 μm); 5 min of field application. [Color figure can be viewed in the online issue, which is available at www.interscience.wiley.com.]

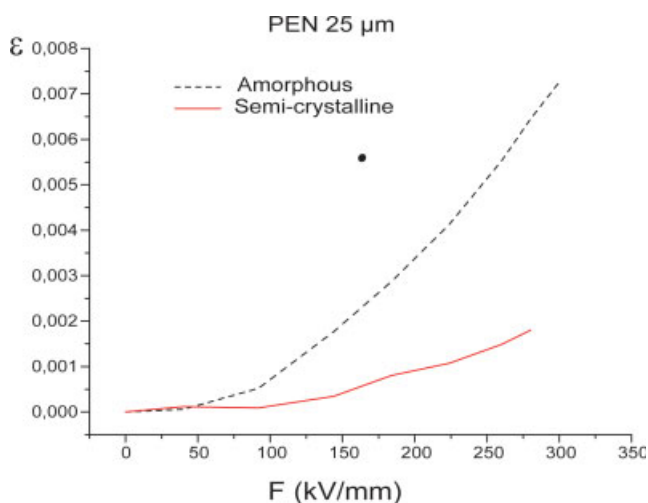


Figure 10 Induced mechanical deformation versus electric field. [Color figure can be viewed in the online issue, which is available at www.interscience.wiley.com.]

It was noted that before attaining the breakdown field strength in some of the tested samples, the rate of deformation tended to diminish once it reached the maximum strain. Work is in progress and the new results concerning this point will be published in a next paper. Figures 8 and 9 show an amorphous sample stressed for 30 min at each voltage step with another 30 min of depolarization between successive stress applications and a semicrystalline sample stressed for 5 min at each voltage step and subjected to the same period of depolarization. The final deformation level is even lower than the levels attained previously at lower electric fields. As a matter of fact, the viscoelastic properties of polymers are reported to change considerably when subjected to high electric fields,⁴ in such way that the elasticity

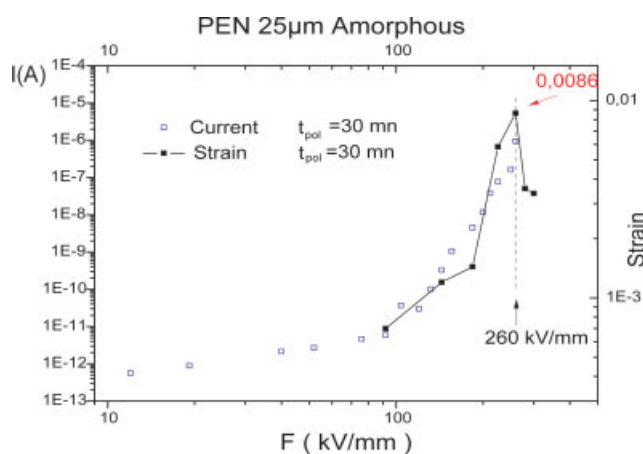


Figure 11 Induced mechanical deformation and conduction current in an amorphous sample versus electric field. [Color figure can be viewed in the online issue, which is available at www.interscience.wiley.com.]

(the storage modulus, G') decreases significantly at a critical field. Hence, this yield point is due to the incidence of field-induced mechanical instability in the polymer morphology (conformational changes). This critical field is quantified, in the cases of amorphous and semicrystalline morphologies, at 260 kV/mm. This is the threshold of critical aging and breakdown in PEN and can be an important reference for practical applications of this polymer. Also, it could be a reference to test other theories related to very high mobility.⁵

Figure 10 shows the deformation versus electric field for both semicrystalline and amorphous PEN samples after 10 min of electrical field application at each level. The shape of the curves in Figure 10 suggests a viscoelastic deformation.^{4,8} The deformation in the amorphous morphology is approximately four times than that of semicrystalline, which is a predictable result because of the effect of crystallinity on the mechanical properties of PEN.^{18–20} Also, this assertion is further supported because of the type of crystallite (β) developed at the surface. The amorphous sample has higher mobility of the chain segments under an electric field which can give an explanation to its threshold field shown in the curves $I(F)$; the semicrystalline case is similar except that the deformation level is lower as well as the resulting current.¹⁵ These are represented in Figures 11 and 12. This molecular mobility probably causes a migration of charge carriers at intramolecular and intermolecular levels.

Also involved are the electromechanical forces in the polymer which increase the conformational change, i.e., the inner space organization of the macromolecule and, consequently, a way for other inter-related processes in the disordered quasi-amorphous interlamellar regions such as the extension of tie

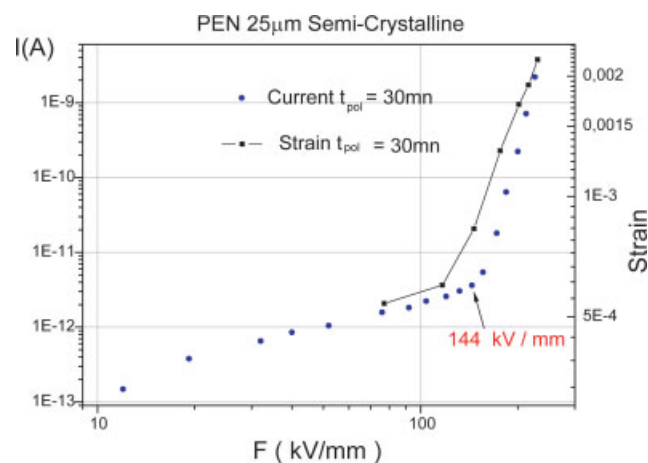


Figure 12 Induced mechanical deformation and conduction current in a semicrystalline sample versus electric field. [Color figure can be viewed in the online issue, which is available at www.interscience.wiley.com.]

molecules and the formation of microvoids. Moreover, the formation of microvoids has been attributed to the scission of the main bonds which produce free radical chain reactions⁸ by affecting the behavior of the current and the threshold field in a significant manner towards the nonlinear zone (quasi-exponential) as well as the breakdown behavior. Indeed, a lot of molecules can swivel internally around one or more of their tie-ups so that during a rotation, they alternate between unstable and relatively stable conformations. Let us presume that there exist conformational preferences coming from the steric effects (Coulombic repulsion and the principle of Pauli exclusion). In addition, the conformational changes will probably vary the molecular interspace (free volume), i.e., the molecular density inside the amorphous zones especially in the vicinity of the inter-phases. These aspects have an influence on the facility or blockage of charge injection.

In fact, local conformational adjustments can result from the possibility of rotation of ester groups with naphthalene, taking into account the obstruction of the various groups fixed on the chain (steric obstruction). However, the conformations taking place can be of large scale depending on the local covalent structure, as also of long distance intramolecular interactions or intermolecular interactions. Already noticed are the formation of the aggregates, the charge transfer complexes (CTC), intra- and intermolecular, which will react to those electromechanical forces to influence the spatial distribution of material or even the mechanisms of conduction between them (the aggregates).

CONCLUSION

The study of the induced mechanical response of PEN 25 μm semicrystalline and amorphous samples subjected to high DC electric fields was conducted using a noncontact optical technique. The results revealed higher deformation levels in case of amorphous samples, i.e., about four times larger. Indeed, the crystallinity and, in particular, the layer of crystallites β on the surface seem to be responsible for this behavior. The resulting deformation levels and patterns were dependent on the level and duration of electric stress application. However, they all start at their respective threshold fields (commencement of deformation) very similar to those presented in the $I(F)$ characteristics (beginning of the nonlinear behavior), in the same material observing same protocols.

Furthermore, a reduction in the deformation rate before breakdown was noticed in some of the tested samples. They show the maximum yield point at the critical field beyond which their deformation rate starts to diminish. This behavior is similar to those reported studying the viscoelastic behavior. The criti-

cal field was quantified to 260 kV/mm, which signifies critical aging and/or the presence of dangerously high mobility carriers.

The breakdown strength levels differed significantly according to the duration of application at each electric stress level. The breakdown could not be assigned alone to an electronic-thermal mechanism or for that matter, to an electromechanical one. It is suggested that a hybrid mechanism incorporating electromechanical cracking and other thermoelectronic processes would be more appropriate. The different breakdown stresses and behavior observed are in favor of such a suggestion.

The authors thank the Regional Council of Midi-Pyrenees, Toulouse, France, the governorat of Alexandria, Egypt, and the program of scientific preparation of the Mexican government called "SUPERA" for providing an opportunity for this research collaboration.

References

1. Blok, J.; Le Grand, D. G. *J Appl Phys* 1969 40, 288.
2. Mamy, P. R. Ph.D. Thesis, Paul Sabatier Université, France, 2004.
3. Mamy, P. R.; Martinez-Vega, J.; Dupre, J. C.; Bretagne, N. *J Appl Polym Sci* 2004, 93, 2313.
4. Jones, J. P.; Lewis, T. J.; Llewellyn, J. P. In Proceedings of the ICSD 2004 IEEE International Conference on Solid Dielectrics, Toulouse, France, July 5–9, 2004; Vol. 1, p 284.
5. Boggs, S.; Kuang, J. *IEEE DEIS*, 1986, 14, 5.
6. Forthergill, J. C. *IEEE Trans Elect Insulat* 1991, 26, 1124.
7. Forthergill, J. C. In Proceedings of 4th International Conference on Conduction and Breakdown in Solid Dielectrics, Sestri Levante, Italy, June 22–25, 1992; p 323.
8. Connor, P.; Jones, J. P.; Llewellyn, J. P.; Lewis, T. J. In the Conference on Electric Insulation and Dielectric Phenomena, October 25–28, 1998; Vol. 1, p 27.
9. Brèmand, F.; Duprè, J. C.; Lagarde, Eur *J Mech A Solids*, 1992, 11, 349.
10. Brèmand, F.; Duprè, J. C.; Lagarde, *Photomécanique* 1995, 95, 171.
11. A. E. Tonelli, *Polymer* 2002, 43, 637.
12. Martinez-Vega, J. J.; Zouzou, N.; Boudouand, L.; Guastavino, J. *IEEE Trans Dielectric Elect Insulat* 2001, 8, 776.
13. Canadas, J. C.; Diego, J. A.; Mudarra, M.; Belana, J.; Diaz-Callaja, R.; Sanchisand, M. J.; Jaimes, C. *Polymer* 1999, 40, 1181.
14. Guastavino, J.; Krauseand, E.; Mayoux, C. *IEEE Trans Dielectric Elect Insulat* 1999, 6, 792.
15. Chavez, J. F.; Martinez-Vega, J. J. In Proceedings of the ICSD 2004 IEEE International Conference on Solid Dielectrics, Toulouse, France, July 5–9, 2004; Vol. 1, p 47.
16. Auge, J. L.; Teyssedre, G.; Laurent, C.; Ditchiand, T.; Hole, S. *J Phys D Appl Phys* 2000, 33, 3129.
17. Chavez, J. F.; Petre, A.; Martinez-Vega, J. J.; Marty-Dessus, D. In Proceedings of the ICSD 2004 IEEE International Conference on Solid Dielectrics, Toulouse, France, July 5–9, 2004; Vol. 1, p 197.
18. Colombini, D.; Zouzou, N.; Martinez-Vega, J. *Macromol Symp* 2004, 212, 479.
19. Hadri, B.; Mamy, P. R.; Martinez-Vega, J. *Solid State Commun* 2006, 139, 35.
20. Zegini, B.; Boudou, L.; Martinez-Vega, J. Presented at the 41st International Symposium on Macromolecules, MACRO2006, Rio de Janeiro, Brazil, July 16–21, 2006.